Application of thermography in diagnosing behavior of metallic materials under dynamic loading conditions

M. Kutin, S. Ristic, M. Puharic
Institute Gosa, Belgrade, Serbia

Keywords

Thermography, welded joints, tension, experimental technique

1. Introduction

With regard to the exploitation safety of the metal and welded structures, the most important are the characteristics, which describe the appearance and growth of the fatigue cracks under the impact of the static and dynamic loads. Welded joint, like complex and heterogeneous structure, presents a critical point in welded structures. The conventional testing methods of the metal structures and welded joints are well known [1]. The properties, obtained by tension tests describe the global mechanical behavior of the materials, especially welded joints.

Thermography is a method which provides the analysis of thermoelastic stress, based on the measurement of infrared radiation, emitted by the component surface, which is exposed to dynamic or static, linear elastic or plastic strain and its conversion into visible image, thermogram [2-11]. Recently infrared thermography has been applied successfully to study the early fatigue behavior of welded steel specimens in laboratory conditions [12]. This non-destructive test typically requires a sensitive infrared camera capable of detecting temperatures changes less than 0.05 mK. In order to calculate the temperature of the monitored object from the radiation reaching the camera sensor and link it with stresses and early fatigue, it is necessary to know emissivity of the object surface, temperature of the surrounding objects, camera distance from the tested object, thermal losses, air temperature and relative humidity [2]. Because of that, it is very difficult to apply infrared thermography for large objects inspection in the exploitation conditions.

Benefits of applying thermography as a non-destructive technique for inspection, monitoring and maintenance surveys of complex structures, operating in the real conditions of the static and dynamic loads, would be better used, if calibration diagrams for construction materials and welded joints exist [13-15].

This paper presents some results relating to making data base of thermographic tests in laboratory condition, on different construction steels and different thechniques welded joints. The experiement and calibration diagrams for: C45E, DX55D and S 355J2G3 steel welded spacemen are presented.

Thermography stands among the different NDT&E techniques, as an attractive tool for fast inspection of large surfaces.

2. Experimental procedure

Experimental set-up for steel specimen's tensile test is illustrated on the Figure 1a, b and c. The testing of specimens was carried out on the electromechanical testing machine, with displacement and the tension control at room temperature. The tension speed was 10 mm/min. The extension was registered using double extensometer. The precision of extensometer measurement is ± 0,001 mm. Tensile testing and thermographic measurements were performed simultaneously.

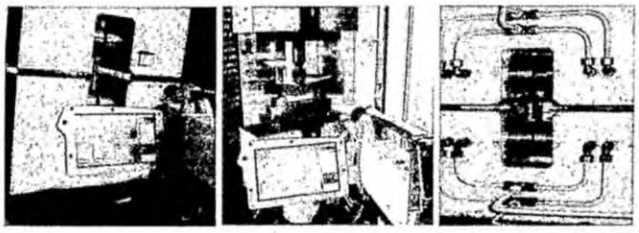

Figure 1. a - Thermographic and tensile test equipment, b - electro mechanical testing machine with crack tip opening displacement (CTOD) control and c - Specimens with a circular hole in RM400

The steels C45E and DX55D are very often used for production of the structures exposed to static and dynamic loads and low temperature action, due to which, in addition to the sufficient strength, its must also have good toughness or ductility. Elements with circular and square cross-section are often integral parts of the structures. For this reason, a series of spacemen C45E with a circular section and DX55D with square section have been investigated.

Welded samples were joined using standard MAG (Metal Active Gas) welding process, designated as 135 according to ISO 4063. Shielding gas (M21) composed of 82% Ar and 18% CO2 (EN 14175) and filler metal W3Si1 (EN 1668) were applied. Samples were investigated by radiography (EN 12517) for joint quality level B (EN 25817). Some tested specimens were removed from the lug assembly of the dredger anchor steel-wire rope Sch Rs 1760/5x32, made of S 355J2G3 steel.

Tensile test of steel spacemen is defined using EN 10002-1 standard. Tests of butt welded joints at room temperature, including the shape and dimensions of the specimens, as well as the testing procedure itself, are defined using EN 895 standard. SE(B) specimens, made of steel S.0563 (S355 J 2 G 3 according to EN 10025), were tested in three-point bending, following the procedures of ASTM E1820, on electro mechanical testing machine, Schenck-treble RM-100, with crack tip opening displacement (CTOD) control, at room temperature. Experimental set-up for structural steel, hole in plate specimen's tensile test is illustrated on the fig. 1c. The

testing of specimens was carried out on the electromechanical testing machine RM400,

The samples have been coated using gray paint with known uniform emissivity, in order to improve their emissive properties.

Therma CAM SC640 Infrared camera, FLIR Systems, has been used for recording thermogram. The camera resolution is 640 x 480 pixels. It was positioned on the distance of 0.5 m related to the sample surface. Camera sensitivity is 60 mK at 30°C, field of view is 24°x18°, minimum focus distance is 0.3 m, spatial resolution is 0.65 mrad, recording frequency is 30 Hz and electronic zoom is 1-8x continuously. Detector type is Focal Plane Array, non-cooled microbolometer 640 x 480 pixels [3]. Camera spectral range is 7.5 to 13 μm, whereas the temperature range is from -40 °C to +1,500 °C, with precision of ±2°C, ±2.

During tests, thermographic camera detected the temperature changes on spacemen surface and made the continuous track. The thermograms, as track sequences, were selected in characteristic time, which was chosen on the stress VS extension curve: force impact start, (elastic strain start), plastic strain start (Yield stress), point where is reached of maximum force, (end of homogeneous plastic strain), up to the final specimen fracture and finally after crack.

For real-time and static image analysis the associated software is used, because it contains powerful measurement and analysis functions for extensive temperature analysis, including isotherms, line profiles, area histograms, image subtraction capability and many more [3].

3. Results and discussions

The testing results are shown simultaneously in order to comprehend the possibilities based on the comparative analysis and to define the criterion for applying the thermography in predictions material behavior during inspection, monitoring and maintenance surveys of complex structures operating in the real conditions of the static and dynamic loads.

3.1. C45E steel spacemen

Detailed analysis of C45E steel spacemen is made to deeply understand the results of simultaneous tests. The geometry and dimensions of spacemen made of C45 E steel are shown in Figure 2 and Figure 3 (upper right corner).

The temperature changes VS time (green line), stress VS extension curves (red lines) and some thermograms for tested spacemen are shown on the fig. 3 for this specimen.

The diagrams (fig. 3) show tensile test results for C45E steel spacemen. In 10th second after test beginning occurs elastically stretching. Temperature curve, a green collared diagram, is almost constant. It varies in the interval 302 ± 0.2 K. The appearance of plastic deformation and the formation of the neck are characterized by appearance of temperature changes with a constant gradient to 18 second and gradient with different slope between 18 and 33 seconds. The total change of the temperature during this interval is ΔT = 23K. In the 34th second, after elongation of 12.5%, spacemen crack occurs. Immediately prior to cracking, temperature rapidly increases to 346K, which gives the total increment of ΔT = 44K. Cooling begins immediately after cracking and after 4 seconds the temperature fall to 316K.

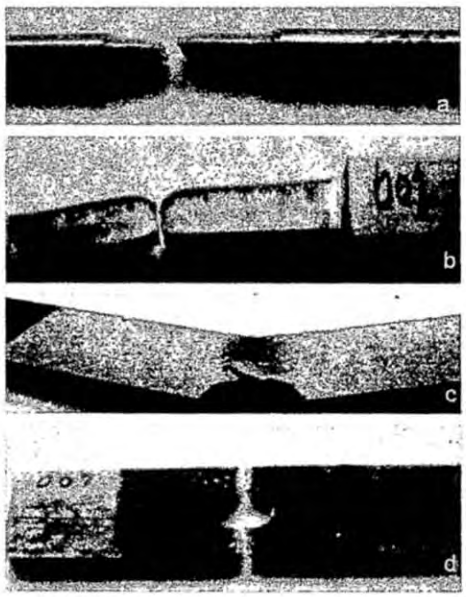

Figure 2. Photo of specimens after tests a - circular crossection, b - rectangular, c - SE(B) specimen and d - specimen with a circular hole

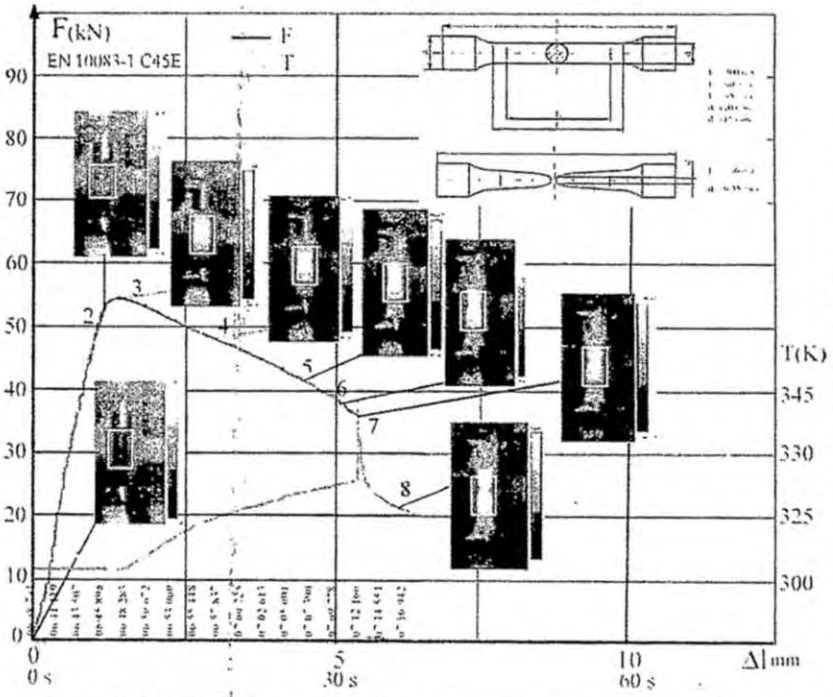

Figure 3. Diagrams of stress VS extension and temperature changes VS time with thermograms in specific points for specimen C45E.

With regard to the testing of steel spacemen, the chart character corresponds to ductile material.

Therma CAM Researcher software makes possible to analyze the temperature in the 640 x 480 point of specimen surface. In the order to analyze temperature variations, two measuring lines were positioned in the middle of the recorded thermograms, L01 vertically and L02 horizontally. The results

are presented on Figure 4. The upper right corner field indicates minimum, average and maximum temperatures at the moment of recording and photo of spacemen after crack.

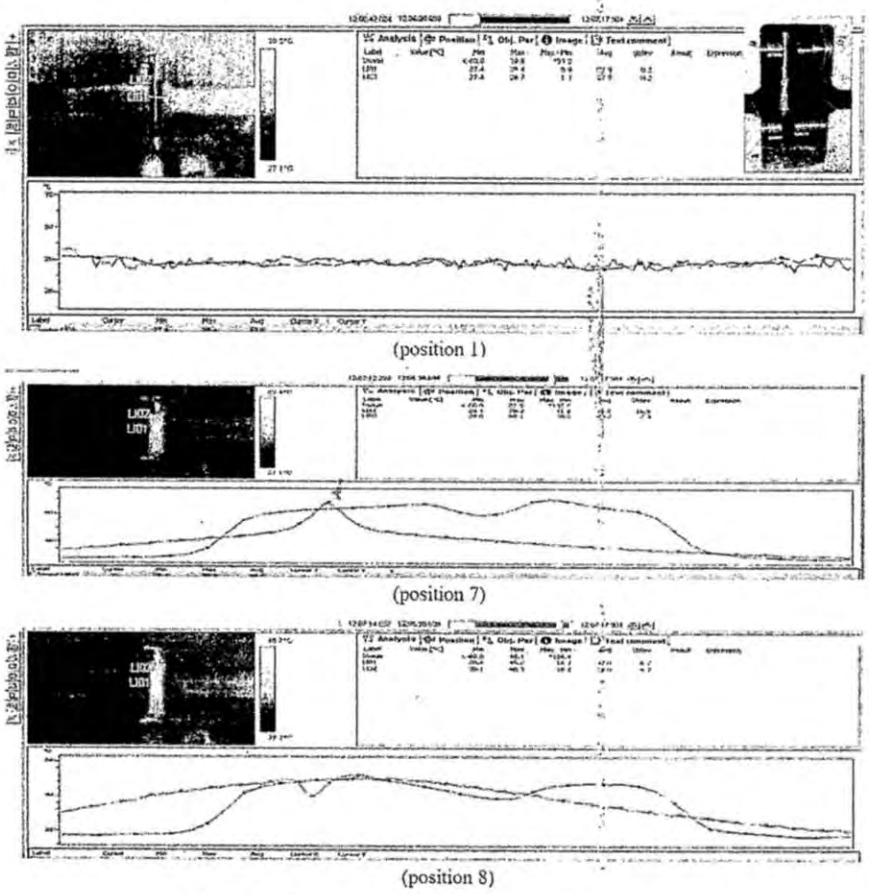

Figure 4. Thermograms and measured temperature values for specimen surface on lines L01 and L02.

Fig. 4 (position 1) shows the temperature at the beginning of test, fig. 4 (position 7) immediately prior to the final cracking, when the highest temperature was detected. Fig. 4 (position 8) shows temperature distribution along lines in the moment when the cooling was began.

The thermograms and the measuring lines on them, illustrate plastic deformations and enable to determine the narrowing cross-section and forming the bar neck. Fig. 3 (upper right corner) shows the dimensions of spacemen cross section before and after stretching. Initial diameter of 10mm was reduced to 6.35 mm (diameter of the neck is about 63.5% of the initial diameter). Horizontal measuring line on the thermogram of spacemen (blue line) is settled to include all the pixels on the test surface. Fig. 4 (position 1) refers to the start conditions. Increased temperature was registered on the line part passing above spacemen surface (that line part includes 14, from a total 22 measuring segments, that is 64% of the total line length). These results are in excellent agreement with dimension measurements. The temperature monitoring during the test in all marked positions provide the detection of the initial temperature variation, indicating where are conditions for initiation of crack under the load impact. Table 1 contains the temperature changes during test. The sudden rising of temperature occurs immediately before cracking.

The crack tip stretching was investigated by scanning electron microscope. Figure 5 illustrates the ductile fracture, record by scanning electron microscopy (SEM), after the tensile test. With regard to the testing of steel spacemen, the chart character corresponds to the ductile, too.

3.2. DX55D steel spacemen

During tensile testing of DX55D steel spacemen, almost 30mm elongation of spacemen is occurred (fig. 3). The experiment lasted about 3 minutes, almost 180s. Thermo camera recorded the images 30 times per seconds; so that the diagram of temperature changes is obtained with 5500 measurements (each thermogram gives one measurement value).

Figure 6 shows diagrams of stress VS extension and maximal temperature VS time on the surface of the sample. Some characteristic points are illustrated with belonging thermograms: the beginning of elastic deformation, then the beginning of plastic deformation, reaching maximum force, the homogeneous plastic deformation to final fracture of spacemen.

Analysis of results presented in fig. 6 shows that in the first 10s the force reaches 42 kN. Temperature of the sample has not changed and elastic deformation occurred with spacemen. Total elongation is 2 mm. The increase in force of only a few kN leads to the appearance of plastic deformation. Max tensile force is about 47 kN. In the time from 12 s to 146 s temperature increases from 305 K to 342 K with a constant gradient, and spacemen total elongation is

Table 1. Temperature variation during tensile test

Spacimen	004
Critical J integral, J_{Ic}, [kJ/m^2]	28.3
The critical stress intensity factor K_{Ic}, [MPa m$^{1/2}$]	79.7
The critical crack length, a_c [mm]	14.2

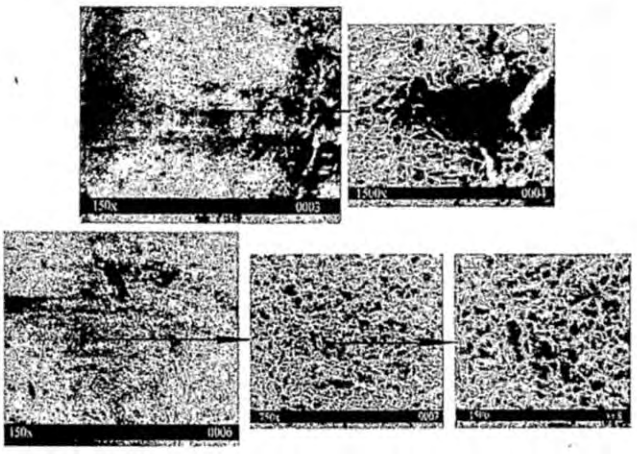

Figure 5. SEM photo of ductile fracture

24 mm. Then, rapidly increase the temperature occurs. 170 s after beginning the spacemen elongation reaches 29 mm. At the same time the spacemen neck is formatted. In 170 s sudden

jump in temperature and spacemen crack occur. After that, the temperature decreases. Diagrams: stress VS extension and maximal temperature VS time; show that the spacemen material DX55D is ductile.

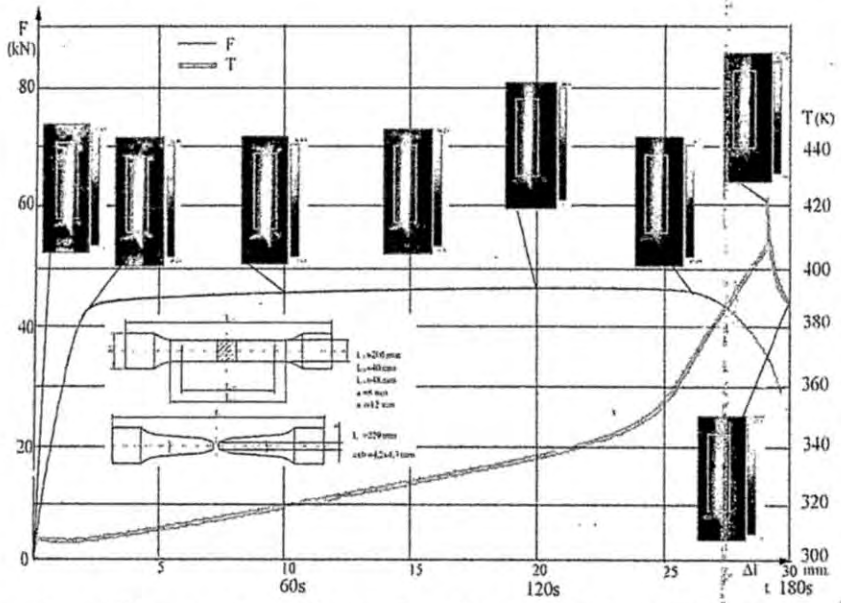

Figure 6. Diagrams of stress VS extension and temperature changes VS time with thermograms in specific points for specimen DX55D

3.3. Welded butt joint specimen

Figure 7 illustrates the diagram of maximum temperature along the surface of welded spacemen versus time. The total time of load impact was 41, 130 s. If the temperature diagram is compared with the stress VS extension diagram of the welded butt joint specimen, it is seen that the significant temperature change hasn't occurred up to the moment which is marked as the position 3 (around 8 s from the start of force impact). In that period the temperature has varied around 303.7 K. The temperature increase has occurred in the point 4. Stress VS extension diagram of the specimen indicates that material leaves the elastic zone and is entering the zone of elastoplastic strains. The temperature change is some ten degrees. The additional temperature gradient occurs in the point 6 (around 20th s). Temperature is increasing faster. The spacemen crack occurs in the point 10. At the moment immediate prior to specimen crack, the temperature increased around 100 K. The cooling occurs after crack (point 11 on diagram).

With regard to the testing of welded joint, the curve character corresponds to the ductile material with approximate participation of homogeneous and non-homogeneous extension in the ratio of 1/2:1/2. The homogeneous extension exists up to the maximum force, whereas the non-homogeneous extension began up to the rupture, i.e. from the moment when the neck is created on the specimen.

The loss of yield stress phenomenon appearance for the specimens of butt welded joint is a consequence of non-homogeneity. The welded joint consists of seam metal, zone of heat affected and basic material. The various microstructures are present in the welded joint as a consequence of different chemical composition and thermal treatment. When the load attains the level when plastic strain should occur (in this case the basic material has the least strength) the appearance of non-linearity occurs.

Crack initiation is a highly localized event which is strongly affected by the random distribution of material properties and defects that exist at the micro structural level. The temperature monitoring during thermographic test provide the detection of the initial temperature changes, indicating where are conditions for appearance and growth of cracks under the load impact.

3.4. SE(B) specimen

Based on data collected from sensors, the diagrams force F - crack tip opening δ (CMOD - Crack Mouth Opening Displacement) were constructed. During the process of crack growth in a specimen in the three-point

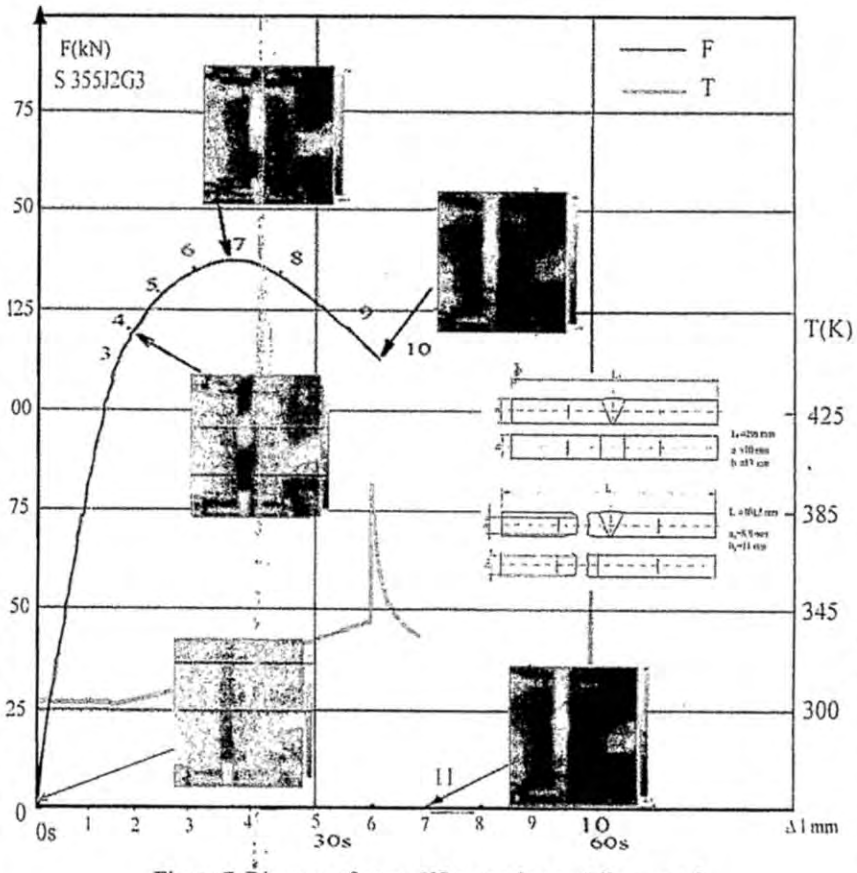

Figure 7. Diagram of stress VS extension and diagram of temperature - time for butt joint specimen

bending test, the temperature distribution on the specimen surface is recorded by thermography. The temperature changes in some characteristic points of the diagram force F - δ opening the crack tip were presented by thermograms.

Table 2. The critical values for 004 specemen

t*	T_{max} [K]	t*	T_{max} [K]	t*	T_{max} [K]
12:06:38.731	302.325	12:06:54.221	310,707	12:07:12.166	323,292
12:06:38.764	302.093	12:06:54.254	310,666	12:07:12.198	323,324
12:06:38.797	302.306	12:06:54.287	310,643	12:07:12.233	323,410
12:06:38.830	302.286	12:06:54.320	310,844	12:07:12.265	323,467
12:06:38.863	302.133	12:06:54.354	310,757	12:07:12.299	345,605
12:06:38.897	302.123	12:06:54.387	310,789	12:07:12.331	344,608
12:06:38.930	302.351	12:06:54.420	310,807	12:07:12.364	340,061
12:06:38.963	302.365	12:06:54.453	310,857	12:07:12.398	336,823
12:06:38.996	302.281	12:06:54.486	310,881	12:07:12.431	334,471
12:06:39.029	302.286	12:06:54.520	311,026	12:07:12.464	332,722
.....	.....	.....	.....	.....	.....
12:06:44.071	302.177	12:06:58.533	314.859	12:07:17.572	316.161
12:06:44.105	302.148	12:06:58.567	314.969	12:07:17.606	316.118
12:06:44.138	302.232	12:06:58.600	314.908	12:07:17.639	316.061
12:06:44.171	302.222	12:06:58.633	314.939	12:07:17.672	316.053
12:06:44.204	302.148	12:06:58.666	315.031	12:07:17.705	316.061
12:06:44.237	302.148	12:06:58.699	315.022	12:07:17.738	316.022
12:06:44.271	302.192	12:06:58.733	315.075	12:07:17.772	316.074
12:06:44.304	302.207	12:06:58.766	315.088	12:07:17.805	316.005
12:06:44.337	302.232	12:06:58.798	315.140	12:07:17.838	316.014
12:06:44.370	302.237	12:06:58.831	315.136	12:07:17.871	315.996
.....	.....	.....	.....	.....	.....
*(hh:mm:ss::xx)					

mechanics - LEML) is called fracture toughness of plane deformation, or the value of stress intensity factor, K_I. The elastic-plastic fracture mechanics (EPML) is focused on the monitoring of crack growth after exceeding the yield strength. In this field as a parameter of fracture mechanics is used moving crack tip, CTOD. The energy parameter of resistance evaluation of the spread of crack in elastic-plastic field is defined by a contour integrals J, which describes the singularity of the crack tip. The critical value of that integral for the first fracture type (splitting) is indicated as J_{IC}, as a parameter of the elastic-plastic fracture mechanics. The dependence of the J integral of the increment crack length presents J-R (or R) resistance diagram and the fracture mechanics parameter which defines the material resistance to crack development. The critical values of fracture mechanics parameters for spacemen 004 are given in the Table 2.

The specimen 004 has a stress concentrator, LT direction. Besides thermograms for t = 0 s, 90 s, 270 s, 330 s and 380 s, the temperature diagrams measured with six line tools in the zone between the point of bending and stress concentrator (Figure 8a) shows the 3D distribution of temperature (Fig. 8b).

The therma CAM Researcher software is capable of measuring temperature at spots, on lines and in selected areas of various shapes and dimensions, as well as of showing isotherms using the gradation of grey or the palette of various colours and shades.

The experimental test results (recorded by fracture mechanics methods and thermography) are shown

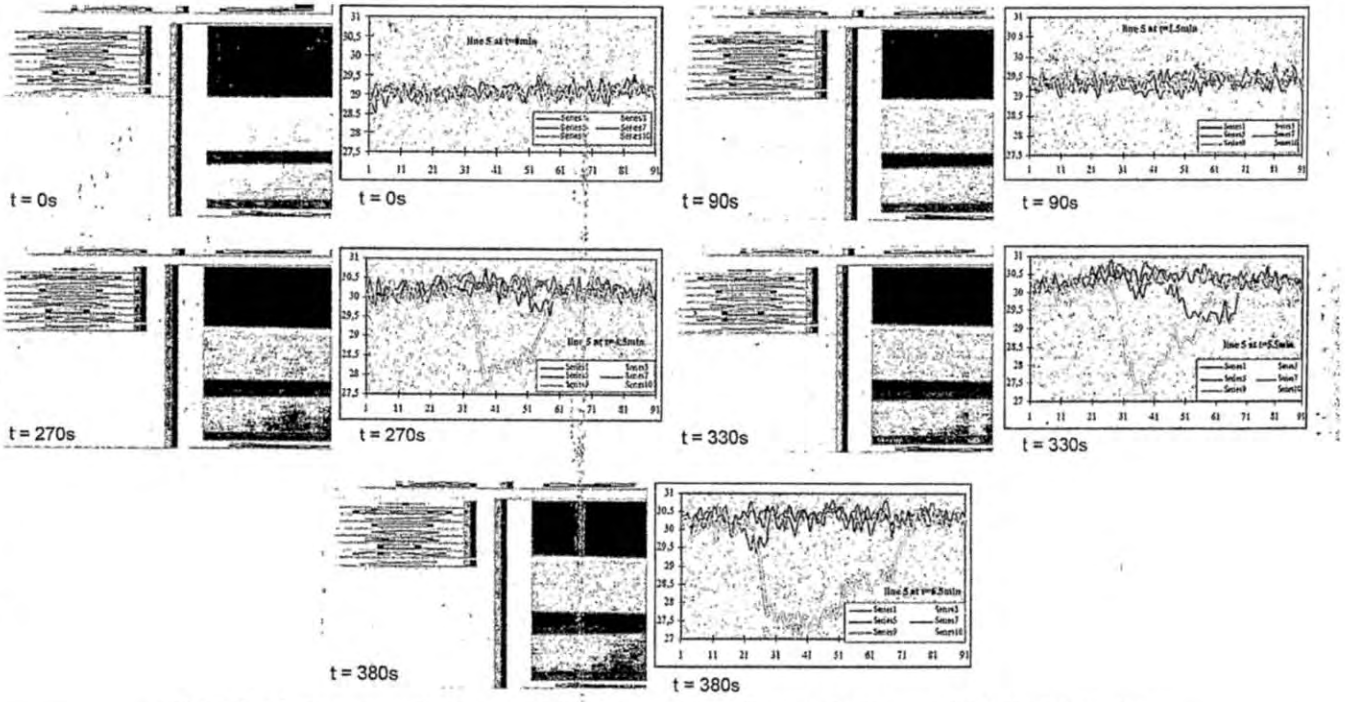

Figure 8. Thermograms of spacimen 004 and temperature diagrams in the zone of plastic deformation

Parameter of fracture mechanics, e.i. the material strength measures in the presence of final size crack in the domain of the Hook's law (linear elastic fracture simultaneously (Figure 9) in order to point out the possibilities based on the comparative analysis and to define a criterion for applying the thermography in prediction of

material behavior, i.e. predicting the initialisation and opening the crack tip.

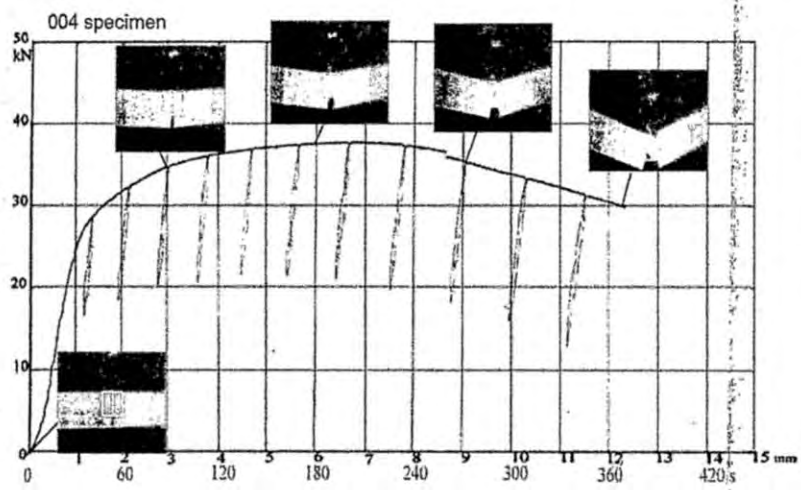

Figure 9. Diagrams of stress vs. extension and vs. time with thermograms in specific points for the 004 specimen

3.5. Specimen with a circular hole

The testing results are shown simultaneously in order to comprehend the possibilities based on the comparative analysis and to define the criterion for applying the thermography in predictions material and plate elements with hole behavior during inspection, monitoring and maintenance surveys of complex structures operating in the real conditions of the static and dynamic loads.

With the help of the Thermo CAM Researcher software, the measuring areas were positioned around the hole of the specimen thermogram, AR01 bellow, AR02 above the hole, AR03 left and AR04 right of hole. For a more precise analysis of the temperature variations on the tested specimen surface and its link to the mechanical properties, the detailed analysis has been conducted into the areas.

The upper left corner presents the recorded thermograms, right corner field indicates the minimum, average and maximum temperatures at the moment of recording. The bottom field contains the temperature distribution into the measuring areas. Figure 10a gives the distribution of maximum and minimum temperatures in the first 14 s after the test start, 10b after 7th s to 22nd s, while 10c gives the same information in same time interval, but only for minimum temperature changing. Fig 10d gives the temperature in marked areas during time interval 14th to 28th s.

The temperature monitoring during the test by thermography, provides the detection of the initial temperature variation, indicating where the conditions for the crack initiation under the load impact are.

The experiment lasted about 28s. to monitor The minimum temperature is monitored on the surfaces AR01 and AR02, while the maximum temperature values in the AR03 and AR04. The tested sample temperature was in equilibrium with the environment. Ambient temperature was 29 °C. Temperatures recorded at the surface of the sample were in the range of 28-30 °C, which is the result of different surface sample emissivity. Fig 10a shows that there were small variations of temperature in the first 18 s of tensile test. After that there was a sudden rise of temperature, on the right side (AR03 to 37.5 °C) and on the left one (AR04 to 32.5 °C). The right side was broken. The temperature on both sides declined to 30.3 °C after 3s. In 22.5th seconds (4.5 seconds after the first fracture of the sample) there was a sudden rise of temperature on the left, to the value of 37 °C and fracture of the sample on the left side (fig 10d). The temperature of the sample was 33.5 °C on both sides of the circular hole after 3 s, and it remained to the end of the test.

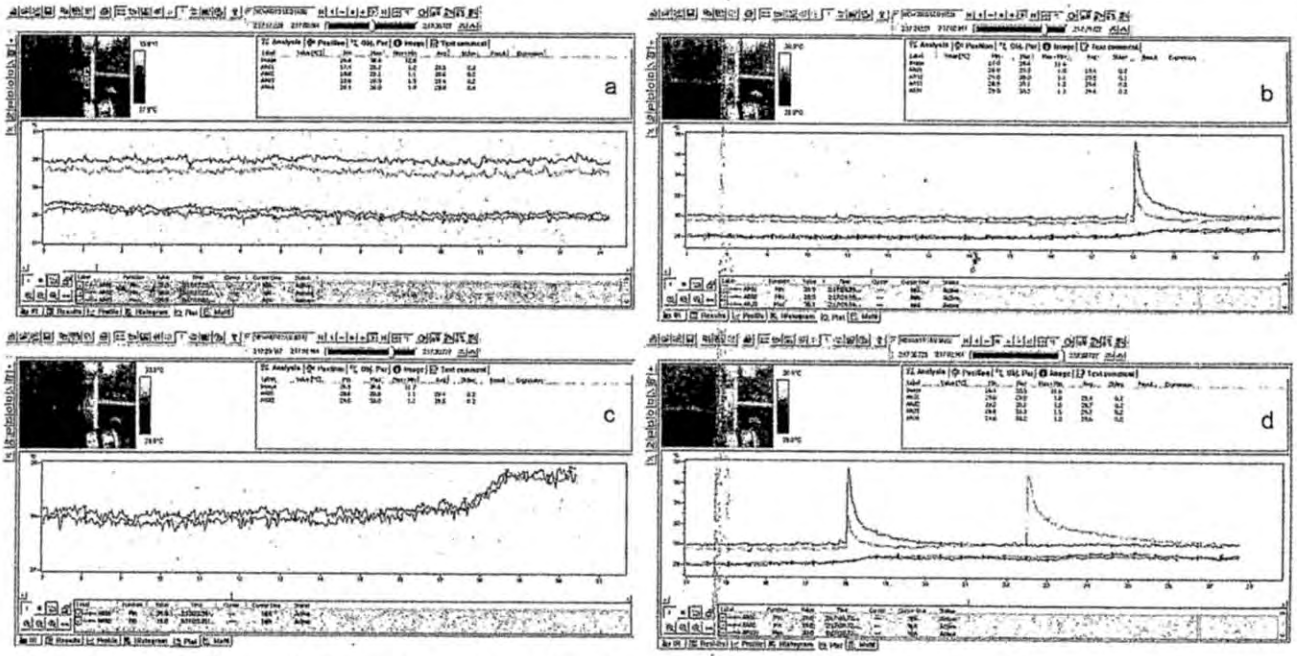

Figure 10. The temperature around the hole on the surface of the structural steel specimen

At the same time, the minimum temperatures in the zones AR01 and AR02 ware changed. The temperature rose from 28 to 28.8 °C at the time of first fracture and that value is retained until the end of the experiment (fig 10c and 10d).

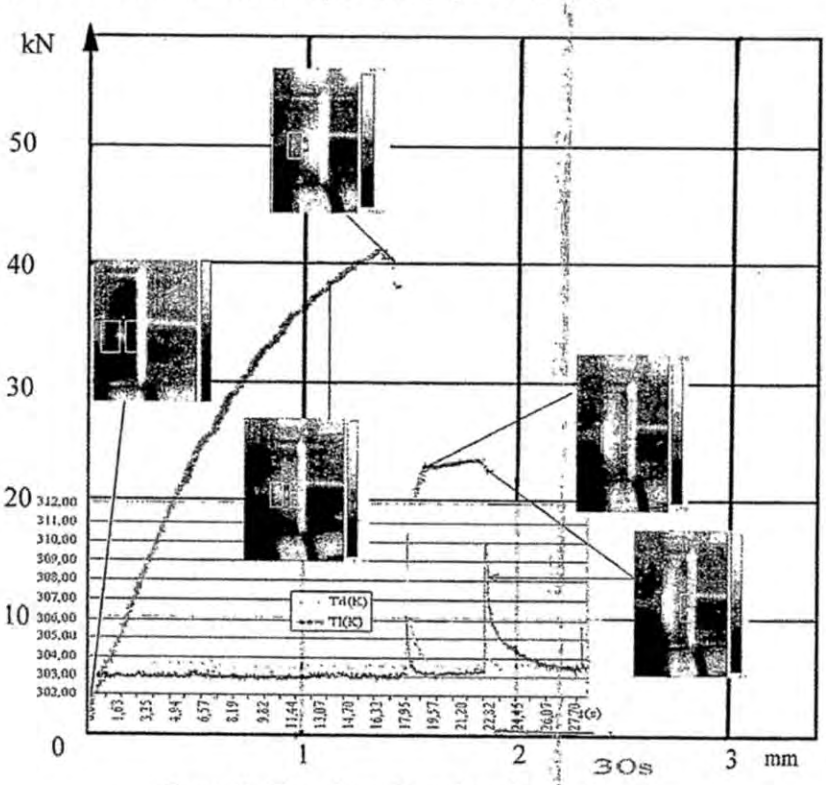

Figure 11. Flow chart of tested specimens with hole

Figure 11 shows the diagrams of stress vs. extension and maximum temperature vs. time on the surface of the sample. Some characteristic points are illustrated with corresponding thermograms: the beginning of elastic deformation, the beginning of plastic deformation, reaching maximum force, the homogeneous plastic deformation to the final fracture of the specimen.

The analysis of the results presented in Fig.11 shows that in the first 18 seconds the force reaches 42 kN. The temperature of the sample was not changed and elastic deformation occurred within the specimen. The total elongation is 1,5 mm. The increase in force of only a few N leads to the appearance of plastic deformation and fracture of right side. The maximum stress in that moment was 8.954 N/m^2. From 18s to 19, 5s, the temperature decreases from 310, 8K to 303, 6K on the right and from 306 to 303, 4K on the left side. The specimen total elongation in 22th s was 1,85 mm. Then a rapid increase in temperature occurs on the left side of circular hole. Immediately before 23th s, the left side was cracked. The total elongation of the sample was 1,9 mm. This value of elongation is measured after the test. Figures 11a-11c show stress distribution for a plate in tension containing a centrally located hole, under applied uniform stress.

It is evident that, crack initiation is a highly localized event which is strongly affected by the random distribution of material properties and defects that exist at the micro structural level. The temperature monitoring during thermography test provide the detection of the initial temperature changes, indicating where are conditions for appearance and growth of cracks under the load impact.

4. Numerical simulation

Stress analysis of some chosen specimens is made with FEM. It is an efficient and reliable numerical procedure for modeling both, linear and nonlinear behavior of materials and structures. Numerical method FEM has been used in order to confirm the ability of thermography to predict the crack of spacemen. Elastoplastic, numerical analysis of the hole in plate made of structural steel is made. The primary aim was to obtain the maximum strain that correspond to the experiment. The model specimens with finite element mesh are shown in Figure 12a and 12b.

Finite element mesh is consisted of 6,178 elements and 11,099 nodes with three degrees of freedom, so the system has a total of 33,297 equations. A global stiffness matrix system of finite element meshes in this case has 33,297 x 33,297elements. Using equations which link displacement and strain, and the equations of deformation and stress, stress distribution is determined. External load were entered into the model on the front surface of the board, while the other plate wedged.

Specimen with the Von Mises stresses is shown in Figure 13.

The highest stress in the plate, around the hole, is $8.83 \cdot 10^8$ N/m^2 (Fig. 13). Numerical results demonstrate a good

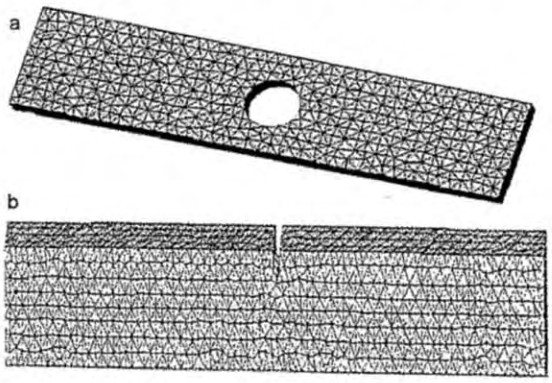

Figure 12. Model specimens with finite element mesh before tensile test, a - specimen with whole, b - SE(B) specimen

agreement with experiment ($8.95 \cdot 10^8$ N/m^2). The static stress concentration factor in the elastic range, Kt, is defined as the ratio of the maximum stress, σ_{max}, to the nominal stress, σ_{nom}. For the infinite plate containing a hole and loaded in tension, Kt = 3. [10]. As the width of the plate decreases, the maximum stress becomes less than three times the nominal stress at the zone containing the hole. Figure 14 shows the point with the maximum stress, where the initiation of crack started.

Finite element mesh for SE(B) specimen is consisted of 7,429 elements and 14,858 nodes with three degrees of freedom, so the system has a total of 456,724 equations. A

global stiffness matrix system of finite element meshes in this case has 23,277 x 23,187 elements. Using equations which link displacement and strain, and the equations of deformation and stress, stress distribution is determined. External load were entered into the model on the front surface of the board, while the other plate wedged.

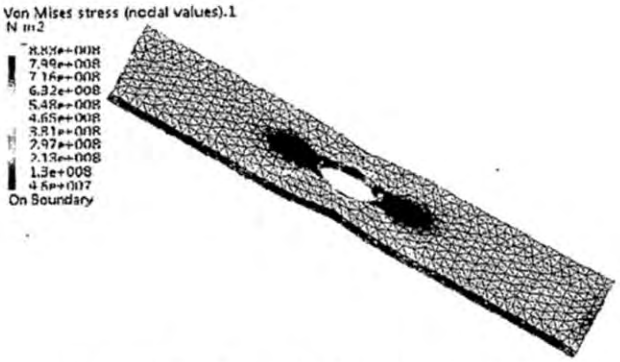

Figure 13. Tensile test simulation, specimen with the Von Mises stresses

- The results, considered in this paper, show that its can be used for someone quickly make a conclusion on whether the temperature increase, sign that critical zone appeared in that place.
- This proves that the variations in temperature captured by the IR camera were strongly correlated to the stress and strain as result of loads applied to the specimens.
- Thermography provides simple and fast location of the defects in the material which could be the spots of the potential cracks initiation and growth.

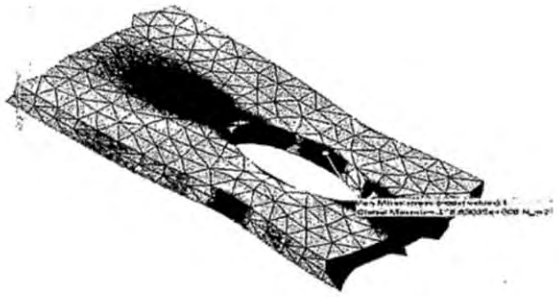

Figure 14. Point with maximum of stress

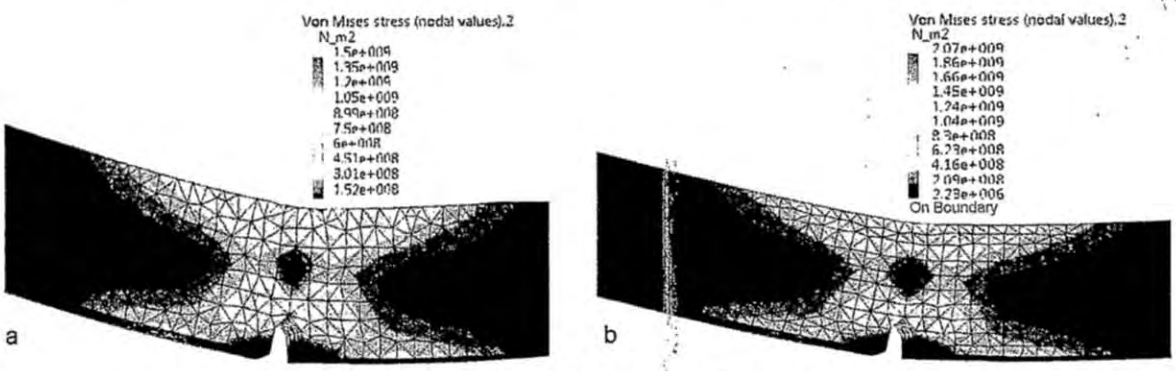

Figure 15. Numerical simulation of test at force of: a - 30 kN and b - 38 kN

Specimen with the Von Misses stresses for test at force of 30 kN is shown in Figure 15a, for test at force of 38 kN is shown in figure 15b.

The highest stress in the plate, around the hole, is $2.07 \cdot 10^9$ N/m^2 (Fig.15). Numerical results demonstrate a good agreement with test results obtain by fracture mechanics.

5. Conclusion

The experiments and results of thermography application, simultaneously with the conventional methods, for testing the tensile properties of metal spacemen and welded joints are presented. The main aim of testing was to relate the temperature changes of the spacemen, continuously recorded by thermography, with stress - extension diagram. As a conclusion can be pointed out that:

- The obtained results confirm that it is very useful to use thermography for early diagnostics of the complex structures in the exploitation or service conditions.
- This technology enables conducting stress analysis and estimation of fatigue limits in a nondestructive and non-contact method within a shorter period. The tensile test allowed obtaining visible data of surface stress distribution using thermography.-This proves that the variations in temperature captured by the IR camera were strongly correlated to the loads actually applied to the specimens.
- Infrared thermography has proven to be an invaluable tool to solve a wide range of scientific questions and problems related to the reliable assessment of the structure integrity and life time.

Acknowledgments

The authors would like to thank the Ministry of Science and Technological Development of Serbia for financial support under the project number TR 34028 and TR 35046.

References

[1] Harwood, N. and Cummings, W.M., Thermoelastic Stress Analysis, 1991. IOP Publishing ltd, Adam Hilger imprint, Bristol, 1991.

[2] Maldague, X.P., Nondestructive evaluation of materials by infrared thermography, Springer-Verlag, London, 1993.

[3] xxx: Flir Systems, The Ultimate Infrared Handbook for R&D Professionals

[4] Luong, M.P., Mechanics of Materials, vol. 28, pp. 155-163., 1998.

[5] Radovanović, R., Milosavljević, A., Kutin, M., Testing a structural member with or without cracks produced of multi-component alloy by applying contemporarily optical techniques, Proceedings, Welding and Joining, Tel-Aviv, Israel, pp. 236, 2005

[6]. Man-Yong, C., Jung-Hak, P., Ki Soo, K., Won-Tae, K., 2006, Proceedings of 12th A-PCNDT 2006 - Asia-Pacific Conference on NDT, Auckland, New Zealand, 2006.

[7]. Bremond, P. and Potet, P., Cedip Infrared System: Application of Lock-in thermography to the measurement of stress and to the determination of damage in material and structures., QIRT conferences 2000.

[8]. Meola, C., Giorleo, G., Nele, L., Squillace, A., Carlomagno G.M., Nondestruct. Test. Eval. 18 (2002) 83-90.

[9]. Krishnapillai, M, Jones, R, Marshall, I.H, Bannister, M., and Rajic, N., Compos. Struct. 67 149-55, 2005

[10]. Meola, C., Carlomagno, G.M., Squillace, A., Giorleo, G., Infrared Physics & Technology 46 (2004) 93-99

[11]. Castanedo, C., Quantitative subsurface defect evaluation by pulsed phase thermography, depth retrieval with the phase, Thèse (Ph.D.), Faculté des sciences et de génie université laval québec, octobre 2005.

[12]. Ummenhofer, T., Medgenberg, J., Int J Fatigue, 31 (2009) 130-137

[13]. Kutin, M., Ristić, S., Burzić, Z., Proceedings. of 3th OTEH 2009, 8-9oct.2009, VTI, Belgrade, Serbia, 2009, IHMTZ/10,

[14]. Song, J.H., Noh, H.G., Akira, S.M., YU, H.S., Kang H.Y., and Yang, S.M., International Journal of Automotive Technology, Vol. 5, No. 1, pp. 55-59, 2004.

[15]. Avdelidis, N.P., Almond, D.P., Marioli-Riga, Z.P., Dobbinson, A., Hawtin, B.C., Proc. Vth International Workshop, Advances in Signal Processing for Non Destructive Evaluation of Materials, Québec City (Canada), 2-4 Aug. 2005. © X. Maldague ed., É. du CAO (2006), ISBN 2-9809199-0-X

[16]. Kutin, M., Ristić, S., Burzić, Z., Testing of butt welded thin steel sheet by classical method and thermography, Proceedings. of 3rd OTEH 2009, 8-9 oct. 2009, VTI, Belgrade, Serbia, IHMTZ/10, 2009

[17]. xxx: http://what-when-how.com/thermomechanics-and-infra-red-imaging/successful-application.

[18]. Diaz, F.A., Yates, J.R., Patterson, E.A., Some improvements in the analysis of fatigue cracks using thermoelasticity, Int. J. Fatigue, 26(4):365-376, 2004.

[19]. Guduru, P.R., Yehnder, A.T., et al. Dynamic full field measurements of crack tip temperatures, Engineering Fracture Mechanics, vol.68, pp. 1535-1556, 2001

[20]. Kutin, M. , Ristić, S., Puharic, M., Vilotijević, M., Krmar, M., Thermographic testing of epoxy-glass composite tensile properties, Contemporary Materials II-1, UDK 66017:621.362.1]: 539.42, pp. 88-93, (2011)

[21]. Haldorsen, L.M., Thermoelastic stress analysis system developed for industrial application, Institute of mechanical engineering Aalborg University, ISBN 82-7644-057-6, 1998

[22]. Kutin, M. , Ristić, S., Puharic, M., Ristić, M., Tensile features of contractual hole in plate specimen testing by thermography and conventional method, Third Serbian 28th Yu Congress on Theoretical and Applied Mechanics, Vlasina lake, Serbia, 5-8 july 2011

[23]. Cozzens, R., Catia V5 version 17, SDC publication, (2008).